Research Article ISSN 2771-666X

Journal of Advanced Materials Science and Engineering

Triboelectric Nanogenerators: From Theory to Experiment

Bejjani Micheline*, Beya Far Aicha and Basset Johnnoel

American University in Dubai, Dubai, UAE.

*Correspondence:
Bejjani Micheline, School of Engineering, American University in Dubai, Tel: +971 4 318 3499.

Received: 30 Aug 2024; **Accepted:** 03 Oct 2024; **Published:** 14 Oct 2024

Citation: Micheline B, Aicha BF, Johnnoel B. Triboelectric Nanogenerators: From Theory to Experiment. J Adv Mater Sci Eng. 2024; 4(2): 1-5.

ABSTRACT

In this study, short circuit charge, current, voltage, and power of triboelectric nanogenerators made of different materials are studied theoretically, guiding to finding optimal material to be used for specific applications. An experiment was performed to validate the theory. Surface defects was a major reason for the deviation from theory as well as the presence of charge leakage and parasitic capacitance not considered in the theoretical studies.

Keywords

Matlab, Oscilloscope measurements, Triboelectric nanogenerators, Vertical-mode.

Introduction

With the focus on environmental sustainability along with the growth in technology, many research fields are emerging. One such field involves harnessing various forms of readily available natural energy for sustainable power generation. Beyond solar [1], wind [2], ocean [3], biomass [4], geothermal [5], hydrogen energy [6], and hydropower [7], ambient energy harvesting [8,9], has become increasingly significant. By devising efficient devices to capture this residual mechanical energy, we can pave the way for generating ecofriendly and customizable electrical energy [10]. Triboelectric nanogenerators, TENGs, offer an innovative solution to the global energy crisis. These devices leverage contact electrification and electrostatic induction to convert mechanical energy into electricity without the need of any external power supply. By harnessing mechanical energy from various sources such as human motion and mechanical activities, TENGs have become a promising technology especially for self-powered sensing system and energy harvesting [11,12]. Their integration with an energy storage device will be crucial for their practical application.

TENGs operate based on charge separation mechanisms, and four working modes have been developed: vertical contact mode, where tribomaterials are vertically moved apart, sliding mode where the tribomaterials are slid apart, single-electrode mode as one electrode moves relative to a stationary surface, and free-standing mode where a free-standing triboelectric layer moves independently between two stationary electrodes [13].

The vertical mode, known for its straightforward structure, has numerous applications as both a power source and active sensor and can be used to collect the energy from activities such finger tapping, running, and walking [14]. This mode will be the focus of our study. In short, two different materials come in contact, and due to the difference in electron affinities, one material will become positively charged and the other negatively charged. At the same time, induced charges will be generated on the back electrode of the two materials. Then, when the two materials are separated, an air gap will be created, resulting in a dipole moment. The electric field generated by the dipole is proportional to the electric dipole moment. If the materials are continuously in contact then separated, then, for a closed-circuit system, a small amount of AC current will be generated. Most materials used for TENGs are dielectric synthetic polymers due to their low weight, resilience, biocompatibility, low cost, and flexibility [15,16]. However, they are non-biodegradable, thus causing air, water, and soil pollution as well as greenhouse gas emissions. Based on the concept of reduce, reuse, and recycle, developing TENGs from recycled plastics and electronic wastes, will contribute to the circular economy and mitigate the harmful impact on the environment. In this work, the output current, voltage, and power of TENGs made of different materials will be studied theoretically, guiding to find an optimal material to be used in TENGs for specific applications. An experiment will also be performed to validate the results.

Basic Theory

Figure 1 illustrates the vertical-contact separation mode. It consists of two dielectric plates stacked face-to-face, with metal layers deposited on their outer surfaces. The plates have same area *A*, thicknesses of d_1 and d_2, and dielectric constants ε_{r1} and ε_{r2}. The distance between the plates, *x(t)*, can be varied by the application of an external force. Upon contact, the inner surfaces of the dielectric materials acquire equal but opposite static charges of magnitude *Q*, with corresponding surface charge densities of magnitude σ . Upon separation, a potential difference *V* is induced between the electrodes, and the amount of charge transferred between the electrodes is equal to the instantaneous charge on each electrode, with opposite signs. Since the size of the dielectric is much larger than the air gap and the thickness of the electrode, it can be assumed that the electric field is due to an infinite electric plate and Gauss's law is used to derive equations of the electric field.

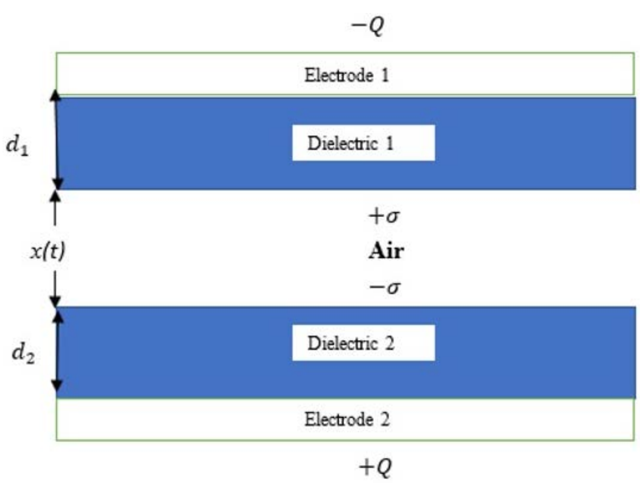

Figure 1: Model of a TENG in vertical mode.

The electric field strength in each region is given by:

$$E_1 = \frac{\sigma_1}{\varepsilon_0 \varepsilon_{r1}} = \frac{Q}{A\varepsilon_0 \varepsilon_{r1}} \quad (1)$$

$$E_2 = \frac{\sigma_2}{\varepsilon_0 \varepsilon_{r2}} = \frac{Q}{A\varepsilon_0 \varepsilon_{r2}} \quad (2)$$

$$E_{air\ gap} = \frac{Q}{A\varepsilon_0} - \frac{\sigma}{\varepsilon_0} \quad (3)$$

The voltage between the electrodes is given by:

$$V(t) = -\frac{Q}{A\varepsilon_0}\left(d_0 + x(t)\right) + \frac{\sigma}{\varepsilon_0}x(t) \quad (4)$$

Where d_0 is function of dielectric constants and thicknesses as seen in equation (5) below:

$$d_0 = \frac{d_1}{\varepsilon_{r1}} + \frac{d_2}{\varepsilon_{r2}} \quad (5)$$

Assuming an open-circuit condition, where *Q = 0*, the open-circuit voltage, V_{oc}, can be derived:

$$V_{OC} = \frac{\sigma}{\varepsilon_0}x(t) \quad (6)$$

For a short-circuit condition where *V = 0*, the short circuit charge, Q_{sc}, can be found:

$$Q_{SC} = \frac{A\sigma x(t)}{d_0 + x(t)} \quad (7)$$

Knowing that the current is the charge per unit time, and assuming the motion of the dielectrics to be linear with a speed *v(t)*, the short-circuit current, I_{SC}, could also be calculated:

$$I_{SC} = \frac{A\sigma d_0 v(t)}{(d_0 + x(t))^2} \quad (8)$$

In the case where the TENG is connected to an external resistor of resistance R, Ohm's law could also be used:

$$V = RI = R\frac{dQ}{dt} \quad (9)$$

Assuming a special case of motion with constant speed, *v*, the top plate will reach a maximum of x_{max} in a time of t_{max} and calculations results are obtained by specifying the below:

$$\begin{cases} x = vt; \ t < \frac{x_{max}}{v} \\ x = x_{max}; \ t > \frac{x_{max}}{v} \end{cases} \quad (10)$$

The analytical solution of $Q(t)$ is:

$$Q(t) = \sigma A[1 - \exp(-Bt - Ct^2) + \sqrt{2}F exp(-Bt - Ct^2) \times Dawson\left(\frac{F}{\sqrt{2})}\right) - \sqrt{2}F \times Dawson(\frac{F}{\sqrt{2}} + \sqrt{C}t) \quad (11)$$

$$B = \frac{d_0}{RA\varepsilon_0} \quad (11.1)$$

$$C = \frac{v}{2RA\varepsilon_0} \quad (11.2)$$

$$F = \frac{B}{\sqrt{2C}} \quad (11.3)$$

$$Dawson(x) = \exp(-x^2)\int_0^x \exp(y^2)\,dy \quad (11.4)$$

The current, voltage, and power as functions of time can be found respectively by using the equations below:

$$I(t) = \frac{dQ(t)}{dt} \quad (12)$$

$$V(t) = RI(t) \quad (13)$$

$$P(t) = V(t)I(t) \quad (14)$$

Simulation Studies

In the simulation below, five pairs of TENGs are chosen with rubber as the negative tribo-pair, of dielectric constant $\varepsilon_{r2} = 4$, nylon, PTFE composite, PMMA with additives, and PES with fillers are taken as the tribo positive pairs with $\varepsilon_{r1} = 7.4, 13, 30, 60$

respectively. The length of each of the plates $d_1 = 5.6 \times 10^{-4}\,m$ and $d_2 = 1.15 \times 10^{-4}\,m$ and their area is $4 \times 4\ cm^2$. The maximum distance between the plate is $x_{max} = 2mm$. It is assumed that the surface charge density of the materials is $\sigma = 20\,\mu C/m^2$ and the resistance $R = 100 \times 10^6\,\Omega$. The short circuit charge, Q_{SC} is plotted *vs x* in figure 2.

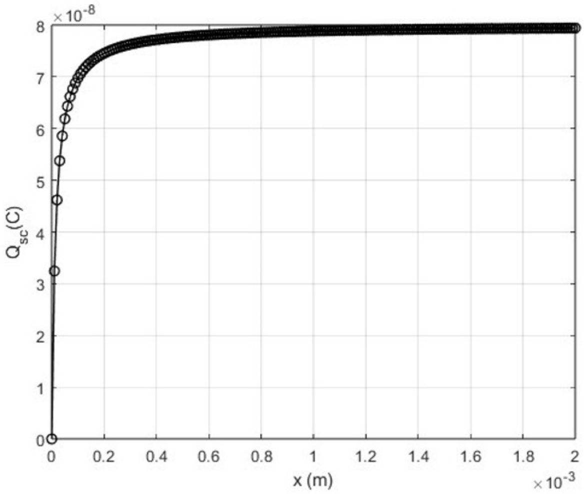

Figure 2: Q_{sc} vs x.

In figure 3, the charge was plotted function of the time. Figures 4, 5, and 6, show respectively the current, voltage and power function of the time. Theoretically, as TENGs were connected to high resistances, there was continuously high voltages because the current flow was minimal.

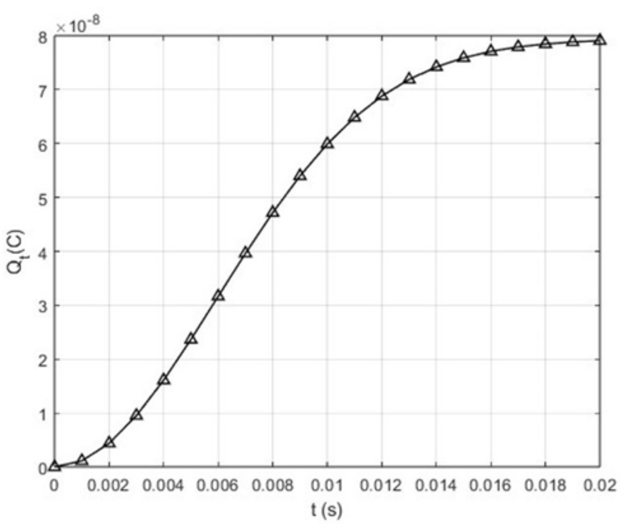

Figure 3: Q vs time.

To validate the theoretical predictions of triboelectric charging, an experiment utilizing the vertical-contact mode was conducted. Six different triboelectric pairs were fabricated and tested in the laboratory. These pairs were constructed from four distinct materials: file plastic, Elle Erre paper, nylon, and Teflon. The specific combinations tested were as follows: file plastic with Elle Erre paper, file plastic with nylon, file plastic with Teflon, nylon with Teflon, nylon with Elle Erre paper, and Elle Erre paper with Teflon. For the experiment, a rectangular bottom base with an area of $6 \times 4\ cm^2$ was prepared. A top base of $4 \times 4\ cm^2$ was centered and attached on top of the bottom base using glue. The triboelectric materials were adhered to the top base using double-sided tape, ensuring that the entire top base area was covered by the material. The separation distance between the materials in each pair was consistently maintained at 2 mm, achieved by placing two sponges on opposite sides of the base. Figure 7 shows a sample of the different triboelectric pairs fabricated in the lab. The contact and separation were performed manually using a single index finger to apply the force. Each triboelectric pair underwent ten trials to measure the maximum voltage, minimum voltage, and the peak-to-peak voltage generated during contact and separation. The average peak-to-peak were measured. Figure 8 shows the pulses on the oscilloscope when the force was applied on the different pairs.

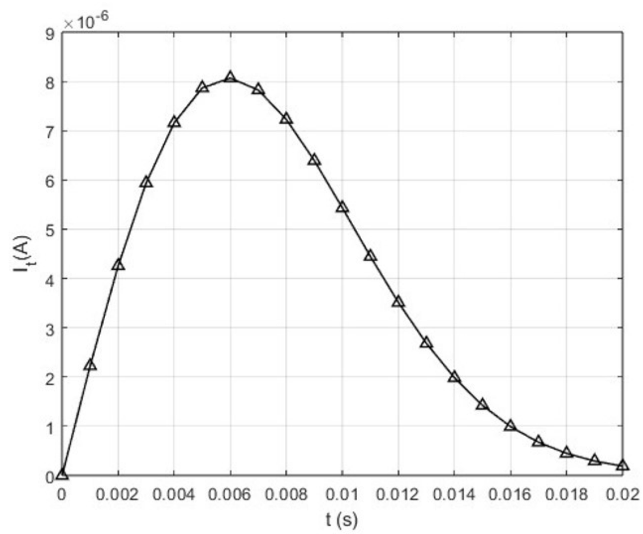

Figure 4: I vs time.

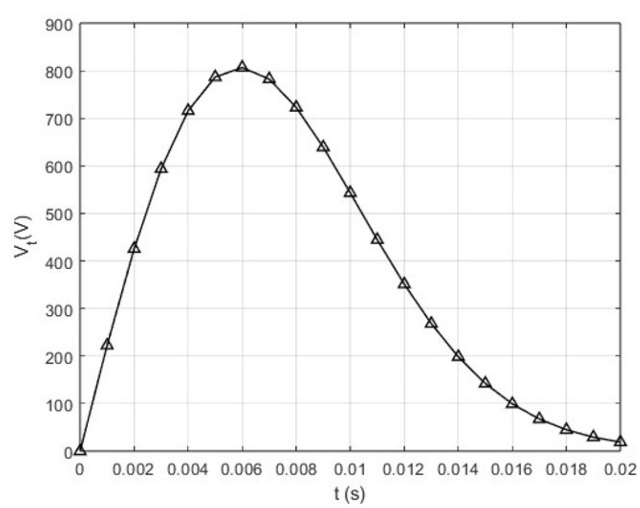

Figure 5: V vs time.

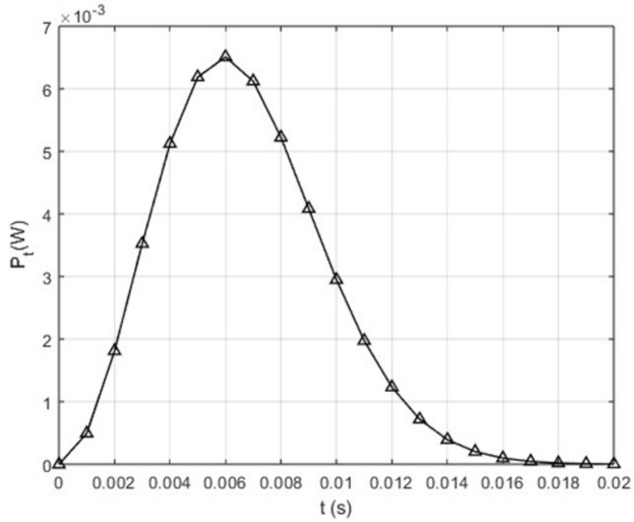

Figure 6: P vs time.

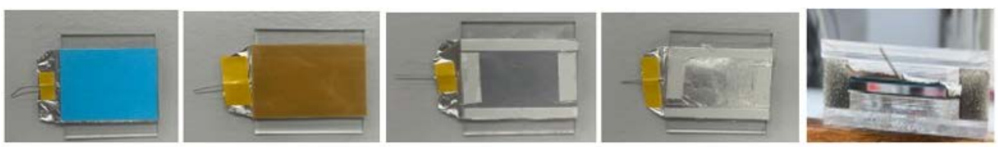

Figure 7: Different samples fabricated in the lab.

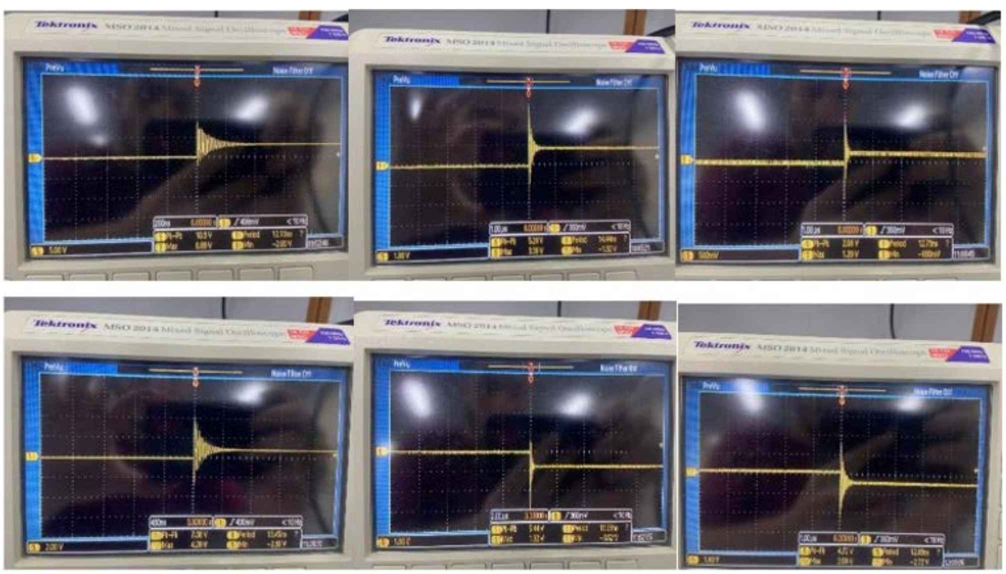

Figure 8: Oscilloscope voltage values for the different samples.

Material	Peak-to-peak voltage (*V*)
File Plastic and Elle Erre Paper	4.098
Nylon and Elle Erre Paper	2.948
Nylon and Teflon	2.368
Elle Erre Paper and Teflon	2.228
File Plastic and Nylon	2.116
File Plastic and Teflon	1.25

Figure 9: Peak-to-peak voltage of the different pairs.

The peak-to-peak average voltage values of the different pairs is summarized in figure 9. In descending order, the materials with the highest average peak-to-peak voltages are the file plastic and Elle Erre paper, nylon and Elle Erre paper, nylon and Teflon, Elle Erre paper and Teflon, file plastic and nylon, and lastly file plastic and Teflon, with average peak-to-peak voltages of 4.098, 2.948, 2.368, 2.228, 2.116, and 1.25 respectively. According to the triboelectric series theory [17], nylon is predicted to charge positively, file plastic to exhibit moderate positive triboelectric charging, Elle Erre paper to be slightly negative or neutral, and Teflon to exhibit strong negative triboelectric charging. As the theoretical maximum triboelectric effect should occur between materials with the greatest tendency to gain or lose electrons, pairs including Teflon with either file plastic or nylon are predicted to produce the highest voltages. The experimental results showed deviations from theoretical predictions based on the triboelectric effect. The highest voltage was unexpectedly produced by the file plastic and Elle Erre pair, indicating that factors beyond simple triboelectric tendencies, including surface roughness and contact mechanics, play significant roles in the triboelectric performance. In fact, experimentally, when pressing with one finger, the contact area and pressure applied are very small, limiting the amount of charge transferred. Contaminants or surface roughness reduced the effective contact area and affected the efficiency of charge transfer. Also, in the experimental set up, charge leakage and parasitic capacitance in the connections and materials reduced the observed voltage. These factors are not considered in the theoretical ideal conditions.

Conclusion

Triboelectricity has been a promising technology for harnessing waste mechanical energy and converting it to a useful infinite power generation source. The study to enhance the output performance of the device is an emerging area. In this work, theoretical simulations were done to find a tribopair providing optimum power. Charge leakage and parasitic capacitance were not considered. After doing an experiment, it was noticed that the results did not validate the theory as surface defects and contaminants played a huge result in effective charge transfer. Surface treatment technology may be an important factor to consider to further improve the power density of the device and to make it more practical.

References

1. Wolniak R, Skotnicka-Zasadzień B. Development of Photovoltaic Energy in EU Countries as an Alternative to Fossil Fuels. Energies. 2022; 15: 662.
2. Ortega-Izquierdo M, Del Rio P. An analysis of the socioeconomic and environmental benefits of wind energy deployment in Europe. Renewable Energy. 2020; 160: 1067-1080.
3. Khan MZA, Khan HA, Aziz M. Harvesting Energy from Ocean: Technologies and Perspectives. Energies. 2022; 15: 3456.
4. Tzelepi V, Zeneli M, Kourkoumpas DS, et al. Biomass Availability in Europe as an Alternative Fuel for Full Conversion of Lignite Power Plants: A Critical Review. Energies. 2020; 13: 3390.
5. Yudha SW, Tjahjono B, Longhurst P. Sustainable Transition from Fossil Fuel to Geothermal Energy: A Multi-Level Perspective Approach. Energies. 2022; 15: 7435.
6. Peng X, Qi Q, Wang X, et al. Recent progress in organic-inorganic halide perovskite solar cells: Mechanisms and materials design. Mater Sci Energy Technol. 2020; 3: 193-202.
7. Panwar NL, Kaushik SC, Kothari S. Role of renewable energy sources in environmental protection: A review. Renew Sustain Energy Rev. 2011; 15: 1513-1524.
8. Ambrożkiewicz B, Rounak A. ENERGY HARVESTING – NEW GREEN ENERGY. J of Tech and Explo in Mech Eng. 2022; 8: 1-7.
9. Zakaria HA, Awal MR, Rahim A, et al. Development of an Ocean Wave Energy Harvester using an Array of Flexible Piezoelectric Sensors. Journal of Advanced Research in Applied Mechanics. 2024; 117: 128-136.
10. Kumar KU, Hajra S, Mohana Rani G. et al. Revolutionizing waste-to-energy: harnessing the power of triboelectric nanogenerators. Adv Compos Hybrid Mater. 2024; 7: 91.
11. Chen B, Wang ZL. Toward a new era of sustainable energy: Advanced triboelectric nanogenerator for harvesting high entropy energy. Small. 2022; 18: e2107034.
12. Zhu J, Zhu M, Shi Q, et al. Progress in TENG technology A journey from energy harvesting to nanoenergy and nanosystem. EcoMat. 2020; 2: e12058.
13. Bu C, Li F, Yin K, et al. Research progress and prospect of triboelectric nanogenerators as self-powered human body sensors. ACS Applied Electronic Materials. 2020; 2: 863-878.
14. Liu L, Guo X, Liu W, et al. Recent Progress in the Energy Harvesting Technology From Self-Powered Sensors to Self-Sustained IoT, and New Applications. Nanomaterials. 2021; 11: 2975.
15. Dzhardimalieva GI, Yadav BC, Lifintseva TV, et al. Polymer chemistry underpinning materials for triboelectric nanogenerators (TENGs): Recent trends. European Polymer Journal. 2021; 142: 110163.
16. Zhao Z, Lu Y, Mi Y, et al. Structural Flexibility in Triboelectric Nanogenerators: A Review on the Adaptive Design for Self-Powered Systems. Micromachines. 2022; 13: 1586.
17. Zhang X, Chen L, Jiang Y, et al. Rationalizing the Triboelectric Series of Polymers. Chemistry of Materials. 2019; 31: 1473-1478.